Integrated Modelling of the Friction Stir Welding Process

Integrated Modelling of the Friction Stir Welding Process

S.W. Williams[1], P.A.Colegrove[1], H.Shercliff[2], P.Prangnell[3], J.Robson[3], P.Withers[3]
D.Richards[3], A.Sullivan[3], N.Kamp[3], D.Richards[3], D.Lohwasser[4] and M.Poad[5]

[1]Welding Engineering Research Centre, Building 46, Cranfield University Cranfield, Bedfordshire, UK, MK43 0AL,

[2]Dept. of Engineering, Cambridge University, Trumpington Street, Cambridge, UK, CB2 1PZ

[3]Manchester Materials Science Centre, University of Manchester and UMIST, Grosvenor Street, Manchester, UK, M1 7HS,

[4]Airbus Germany,

[5] Airbus UK, Filton, Bristol, UK, BS99 7AR

SYNOPSIS

In any welding process it is desirable to use modeling to reduce the time for process optimisation and increase the amount of process innovation. Ideally the model would take input process parameters and produce outputs in terms of joint performance. This requires an integrated modelling approach incorporating coupled process, material response and material performance models. This paper provides details of how this is being implemented for use in friction stir welding for application to aerospace structures. Currently the process model is a dynamic coupled fluid flow thermal model. The material response models comprise microstructural and residual stress models. The material performance models are targeted at mechanical properties, corrosion behaviour and fatigue performance. The paper highlights the state of development of each of the sub models and the degree of coupling together that has been achieved.

1 INTRODUCTION

A user of FSW modelling would like to input material and process parameters and have as output joint performance predictions as shown in Fig 1.

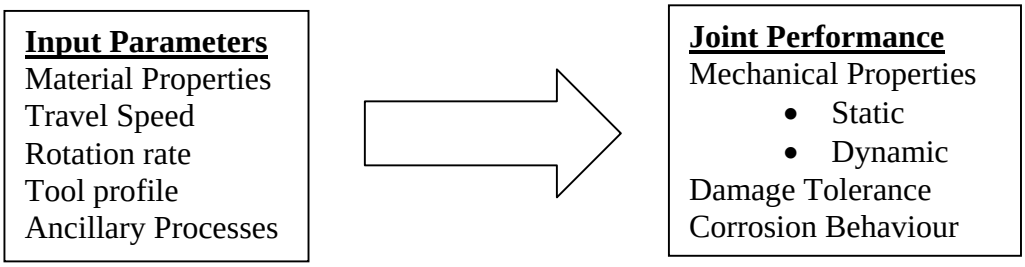

Fig. 1 Requirements for a friction stir weld process model from a user's standpoint

To achieve this level of sophistication an integrated modeling approach is required and Figure 2 shows the sub-models required.

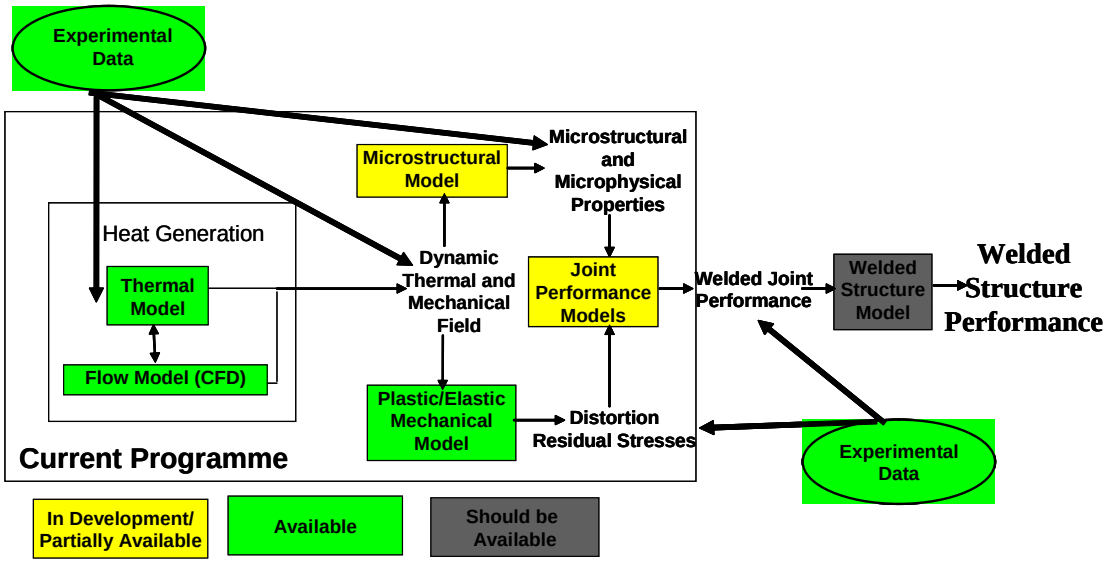

Fig 2 Elements required for an integrated FSW model

As seen in Figure 2 several sub-models have been independently developed and then coupled together. Experimental data is used for validation of individual models and to allow independent development of any sub-model. For each model stage there may be several different models available depending on the level of detail required and the processing time that is available.

2 MODEL DESCRIPTIONS AND EXAMPLE OUTPUTS

2.1 Heat Generation

For representation of the basic FSW process three modelling approaches have been adopted:

1. Simple thermal modelling utilising a bespoke finite volume code, TS4D, developed at Essex University (1). This approach neglects any deformation effects but gives accurate thermal profiles but requires experimental thermal data to adjust the heat source profile
2. Full FE flow modelling has been developed and applied to FSW (2, 3). The predictions have been shown to be useful but the model takes a long time to run.
3. A coupled 2D flow and thermal field model has been developed and this is used as the basic heat generation model for the integrated model (4).

The coupled 2D flow and thermal field model was developed to predict weld heat generation and temperature from the flow and thermal properties of the material being welded, the tool and plate dimensions and the process parameters. The modelling approach involved coupling a 3 dimensional thermal model for calculating the heat flow to a 2 dimensional axisymmetric flow model for calculating the heat generation. A flow diagram showing the coupling between these two models is shown in Fig 3. The 'Translating 3D Thermal Model' is solved in steady-state and predicts the temperature field around the tool from the heat flux applied at the tool-workpiece interface. This model captures the effect of tool translation. An averaged temperature field from this

model is then imposed on the domain of the '2D Axisymmetric Flow Model'. The temperature affects the flow strength or viscosity of the material in the 2 dimensional model. The '2D Axisymmetric Flow Model' calculates the flow of material through a cross-section underneath the tool shoulder which is shown in Fig 3. This model is solved and the effective heat flux across the tool surface is found from the material flow strength. This heat flux is imposed on the 'Translating 3D Thermal Model' which is then solved using the updated heat flux. The process is repeated until the solution converges, i.e. there is no further change in the heat generation, temperature and flow fields. The starting point for the calculation is an isothermal temperature distribution of 500°C.

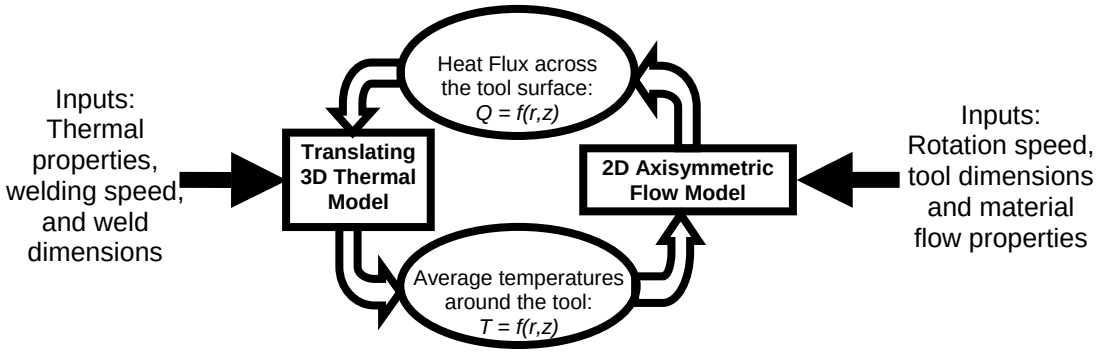

Fig 3 Flow diagram showing how the 2 dimensional axisymmetric flow model is coupled to the thermal model

To illustrate the usefulness of the model, the heat generation of 2024-T3 and 6013-T6 shown as a function of welding and rotation speed are plotted in Fig 4(a). In both materials the heat generation rises to a plateau with increasing rotation speed. This characteristic is also observed experimentally. It is suggested that the 'ideal' rotation speed is at or just before the plateau in the heat generation. This corresponds to a rotation speed of 800-1000 for 2024 and 1200-1600 rpm for 6013. Interestingly, this rotation speed also corresponds to the minimum in traversing force. This effect is illustrated in Figure 4(b) which shows the heat generation, traversing force and peak temperature at the shoulder and root of the weld as a function of the rotation speed for a welding speed of 400mm/min.

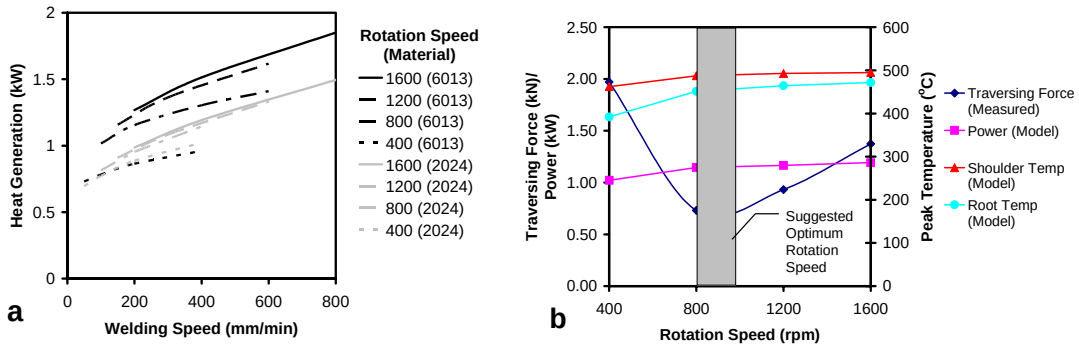

Fig 4 (a) Comparison of the heat generation between 3.2 mm thick 2024-T351 and 6013-T6 welds and (b) plot of the heat generation, traversing force and peak temperatures at the shoulder and root of the weld as a function of the rotation speed for a

welding speed of 400 mm/min using 2024 aluminium alloy

In addition to predicting the heat generation, the 2 dimensional axisymmetric flow model also predicts the rotational flow around the tool, ignoring the tool translation. Figure 5 compares the rotational flow field two welding conditions; rotation speeds of 1600 rpm and 400 rpm at a travel speed of 200mm/min. The rotational flow diagrams are compared with the advancing side of the weld macrosections for the two rotation speeds. These models used the 2014 properties and a slip boundary condition at the shoulder. The comparisons are good, with the model predicting the smaller deformation region under the shoulder with the low rotation speed

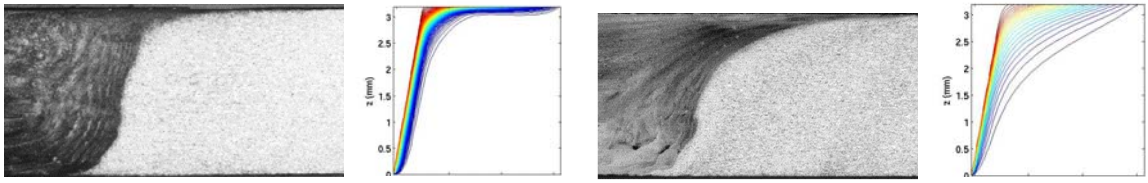

Fig 5 Weld macrosections and corresponding rotational flow diagrams from the welds that used a welding speed of 200mm/min and rotation speeds of (a) 1600 rpm and (b) 400 rpm. The models use the 2014 material properties, and a slip condition at the shoulder

2.2 Residual Stress Modelling

For residual stress modelling the approach is a standard elastic-plastic modelling using the ABAQUS FE platform (5, 6). This approach has been shown to produce good predictions of residual stress profiles for FSW as shown in Fig 6a) which compares the predicted and measured longitudinal stress profiles for AA7449 with welding parameters of a rotation rate of 255rpm and a travel speed of 250mm/min. The model can account for the effect of auxiliary processes such as mechanical tensioning during welding. Fig 6b) shows the predicted longitudinal residual stress profiles for welds made in AA2024 with a welding speed of 195mm/min and a rotation rate of 770rpm with varying levels of longitudinal stretch applied during welding.

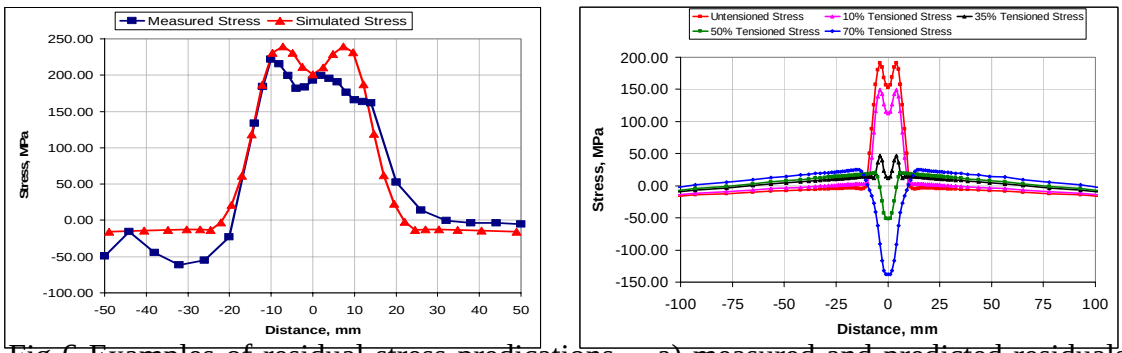

Fig 6 Examples of residual stress predications - a) measured and predicted residuals stress profiles in AA7449 b) predicted residual stress profiles in AA2024 with varying levels of mechanical tensioning applied

2.3 Microstructural Modelling

The microstructural model attempts to accurately predict the evolution of the size, number, and distribution of precipitate particles. Full details of how this model works are available elsewhere (7, 8); the key points are summarized below.

The model is based on the numerical precipitation simulation method developed by Kampmann and Wagner (KWN model) (9). This describes the full particle size distribution evolution and is particularly suited for modelling non-isothermal treatments. Precipitate formation, coarsening and dissolution are all naturally accounted for. The method is based on classical kinetic theory, within a numerical framework, and has been applied with some success to fusion welding of commercial aluminium alloys (10). However, these models approximate multicomponent alloys by pseudo-binary systems and considered only one precipitate phase. Precipitate evolution during welding is a more complex problem where both heterogeneous and homogeneous precipitation sites must be considered, with several phases involved. Furthermore, the metastable phases act as nucleation site for the equilibrium phases, and this needs to be accounted for to predict the microstructures typically seen in welds.

The model reliability and accuracy is dependent on knowledge of the phase equilibria in the alloy system. Thermodynamic properties of the material such as equilibrium solubilities and driving forces are used in the model constitutive equations. The thermodynamic database software JMatPro (11) developed by Sente Software, UK, was used to calculate phase stabilities and equilibrium compositions for both the metastable and equilibrium phases. The model has so far been applied to 7xxx alloys where η' and η are the main precipitate phases. Two types of nucleation are considered in this model (i) direct nucleation of η' and η (both homogeneously and heterogeneously) and (ii) nucleation of η from η' particles. The model is numerical, and the microstructural evolution is calculated by taking small steps in time, recomputing the precipitate distributions and solute levels in the matrix, and using the new microstructural state as the starting condition in the next time-step. A flow chart for this process is shown in Fig 7

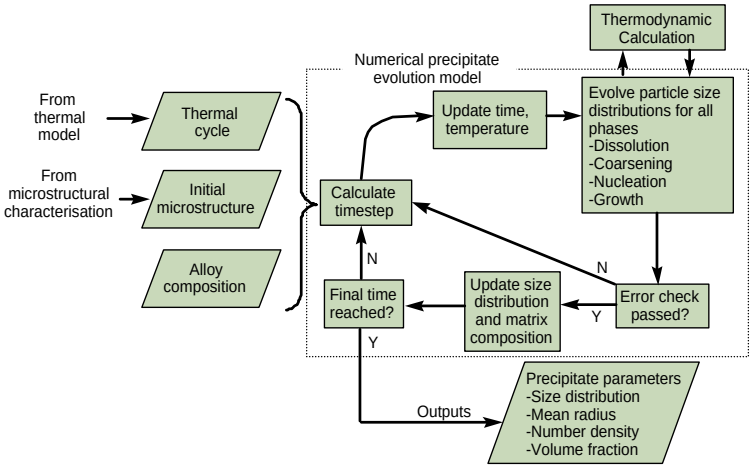

Fig. 7 Flowchart showing the operation of the numerical microstructural evolution model for FSW

Figure 8 shows the predicted evolution of precipitate phases in a AA7449-T7 weld. It is assumed that in the overaged starting condition, the initial microstructure consists of equilibrium η precipitates (with a mean equivalent radius of 4nm). The model predicts that during the weld thermal cycle, partial dissolution of the smaller precipitates will occur, reducing the volume fraction. The extent of dissolution is greatest in the nugget, where the maximum temperatures are reached. On post-weld cooling, it is predicted that η phase will precipitate. However, the final volume fraction reached remains significantly below the initial volume fraction, particularly in the nugget and Thermo-mechanically affected zone (TMAZ). During this time, the mean particle size is increasing as a result of both coarsening of pre-existing particles and precipitation of new particles. The model also predicts a small amount of fine metastable η' forms towards the end of cooling.

These predictions are qualitatively in agreement with the observed microstructures. Large and small precipitates typically characterize the nugget, and the model suggests that these are a mixture of some remnant original (heavily coarsened) particles and other new (smaller) particles formed on cooling after welding.

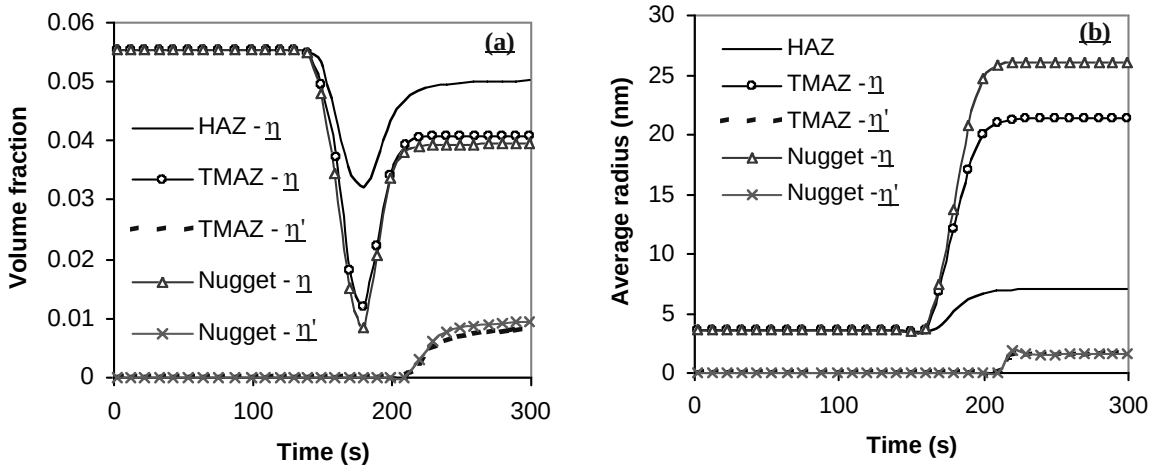

Fig. 8 Predicted evolution of (a) precipitate volume fraction and (b) equivalent radius in AA7449 FSW for three positions typical of the nugget, the thermo-mechanically affected zone (TMAZ), and the HAZ.

The intention is to use the output from the microstructure model to predict corrosion, toughness etc. The microstructure model has been selected to be the most efficient method of capturing the minimum detail required for this to work. i.e. precipitate size, type, density, and heterogeneity (i.e proceeding parameters at grain boundaries and in the matrix), plus the solute level remaining in solution after welding.

2.4 Joint Performance Modelling

There are several aspects to joint performance modelling that are required as follows

1. Mechanical
    - Strength, hardness and ductility
    - Fatigue
2. Damage Tolerance
    - Fracture Toughness
    - Crack initiation and growth
3. Corrosion

Work has started on hardness and fracture toughness models. The first approach for the hardness model is to couple a thermal model to an empirical hardness model. This circumvents the need for the detailed microstructural model but requires calibration for each alloy type. Full details of the hardness model, both in its original version as applied to fusion welds (12), and modified versions applied to FSW are given elsewhere (13-16). A summary of the model is given below.

The model is applicable to alloys which are initially in the peak aged, or overaged conditions. It is based on the assumption that the heat input by the welding process will lead to a strength loss by dissolving strengthening precipitates. Although this is an over simplification of the true microstructural changes (where precipitate coarsening also plays a key role), this is in part compensated for by an experimentally based calibration procedure which implicitly accounts for other effects (16).

To apply this model to welding, it is necessary to calculate an effective equivalent isothermal heat treatment time for the weld cycle. This can be done by considering the thermal cycle as a series of infinitesimal isothermal heat treatments. Once an effective isothermal time has been calculated, a kinetic “master curve” derived from experimental isothermal heat treatments is used to look up the expected as-welded hardness. There is an additional complication because after welding natural ageing will occur, leading to a hardness increase. The amount of natural ageing is greatest in regions of the weld that have experienced the highest peak temperature. In these regions, the maximum precipitate dissolution will have occurred, and the solute in the matrix available for natural ageing will be at a maximum. The natural hardness increment after welding is determined from a measurement of the natural ageing hardness increment after isothermal treatments, assuming that the natural ageing response will be the same as for an isothermal treatment corresponding to the peak temperature reached during welding.

When the simple hardness model is combined with a process model to predict the thermal cycle during welding it becomes possible to predict the hardness variation across welds and hardness maps both before and after natural ageing. Predicted hardness profiles (Fig 9) and maps (Fig. 10) can be produced, and these compare well with experiments. The predictions shown are for AA7449, but the model has been shown to work equally well for AA6013-T6 and AA2024-T6 welds.

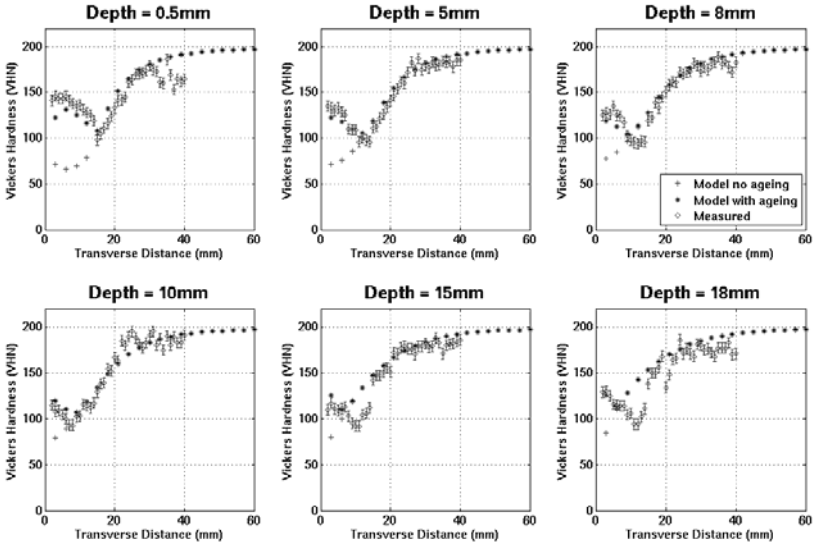

Fig. 9 Predicted and measured hardness profiles as a function of depth from the top surface of the 7449 weld.

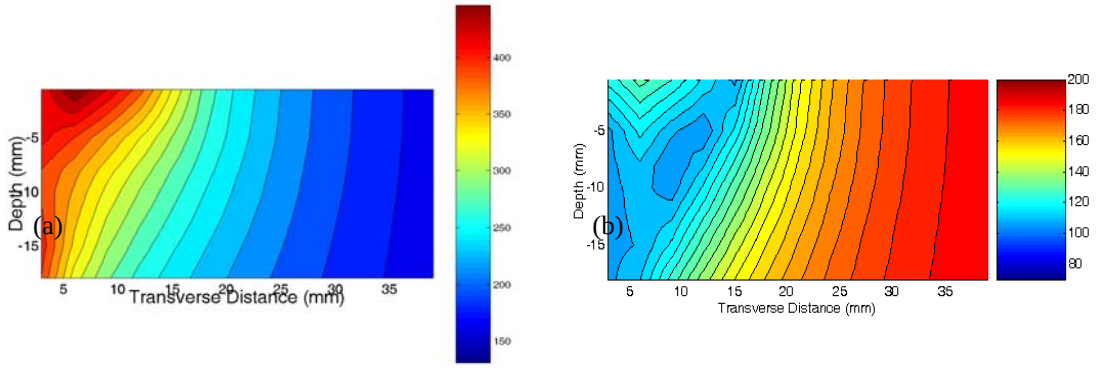

Fig. 10 (a) Predicted peak temperature map for the AA7449 weld (the weld centerline is at traverse distance = 0). (b) Predicted hardness map for the same weld.

Work is currently in progress to link the detailed microstructural predictions available from the numerical precipitation model, as described previously, to models for key properties. Strength has already been modelled successfully [11] and the model is now been extended to more complex properties, including fracture toughness.

The microstructure model provides the necessary microstructrual detail for input into existing fracture toughness models (e.g. [17]) such as precipitate free zone width, and precipitate sizes on the grain boundary and grain interior. These models have been applied successfully to predict toughness in 7xxx alloys subject to quenching under different conditions.

The fracture toughness models also require some mechanical property information, such as the local work hardening exponent, and work is in progress to characterize these variables using tests on material with simulated weld microstructures. Characterization of fracture mode and generation of a set of toughness data for weld-like microstructures has been performed, and this data will eventually be used to test the model.

3 INTEGRATION

When this work began each of the modelling activities was being independently pursued. The direct involvement of a potential user provided a focus and brought these activities together with a view to developing a fully integrated FSW model. Consequently the different research teams have been fully collaborating to try to achieve this ambitious goal. To achieve full integration the models should run on the same software platform, COMSOL Multiphysics was selected for this. Currently the heat generation models (excluding the full FE fluid flow), the microstructural model and the hardness model have been implemented on this platform. The models have been implemented with a graphical user interface. It is intended that other models will be added when developed.

4 FUTURE DEVELOPMENTS

Work to-date has proceeded through a desire to collaborate and to develop an integrated model. This collaboration is shortly to become more formal through the commencement of a UK Dept. of Trade & Industry project entitled Friction Stir Integrated Modelling (FSIM). This project will continue on the development and integration of the models described above. In addition new developments will include the following

1. Crack growth behaviour – welding has a major influence on the behaviour of cracks in metallic structures. This is either through changes in mechanical properties or through induced residual stresses. Modelling of this influence is important to both the understanding of fatigue behaviour and from the damage tolerance aspects.
2. Corrosion modelling - the large changes in microstructure induced by FSW has a significant impact on the corrosion behaviour. Models are needed that predict this change in behaviour so that attempts can be made to optimise the process parameters for improved corrosion properties of welded structures.
3. Statistical modelling – for some scenarios or applications models based on physical principles may not be appropriate, either because of extended run times, poor physical data or general inaccuracies. As an alternative statistical or empirical models will be investigated.

5 CONCLUSIONS

A fully integrated modelling approach for FSW shows the potential to be able to take inputs such as material properties and process parameters and provide outputs of direct interest to the user such as weld joint performance. The integrated model requires the development of several sub-models to be developed which need to be coupled together. Several of these models have already been developed and integrated including the following elements:

- Heat generation
- Residual stress
- Microstructure development
- Hardness prediction

These models have been integrated on a common software platform and provide the user with a single input/output process. Work is continuing on these models along with the development of other joint performance models.

ACKNOWLEDGEMENTS

This work was supported by EPSRC, the Isaac Newton trust and Airbus.

REFERENCES

(1). A.Mackwood, 'Numerical Solution of Thermal Processes and Welding', PhD Thesis, Essex University, 2003

(2). P. A. Colegrove and H. R. Shercliff: 'CFD Modelling of the Friction Stir Welding of Thick Plate 7449 Aluminium Alloy', *Sci. and Technol. Weld. and Joining.*, (in press).

(3). P. A. Colegrove and H. R. Shercliff: '3-Dimensional CFD Modelling of Flow Round a Threaded Friction Stir Welding Tool', *Journal of Materials Processing Technology*, 2005, **169**, 320-327

(4). P. A. Colegrove and H. R. Shercliff: 'A Model for Predicting the Heat Generation and Temperature in Friction Stir Welding from the Material Properties', Sci. and Technol. Weld. and Joining., (Submitted).

(5). D.G Richards, P.E. Prangnell, P.J. Withers, S.W. Williams, A. Wescott and E.C Oliver: 'FE Modelling of Mechanical Tensioning for Controlling Residual Stresses in Friction Stir Welds', THERMEC. Vancouver, Trans Tech Publications, 2006.

(6). D.G Richards, P.E. Prangnell, P.J. Withers, S.W. Williams, A. Wescott and E.C Oliver, 'Geometry Effects when Controlling Residual Stresses in Friction Stir Welds by Mechanical Tensioning', ECRS7. Berlin, Trans Tech Publications, 2006.

(7). N. Kamp and J. D. Robson. TMS Letters, 2 p.1, 2005.

(8). N. Kamp, R. Tomasi, and J. D. Robson, Acta Mater., 54 p. 2003, 2006

(9). R. Kampmann and R. Wagner. Materials Science and Technology, vol. 5. VCH Weinheim, R. Kampmann and R. Wagner. Materials Science and Technology, vol. 5. VCH Weinheim, Germany, 1991.

(10). O. R. Myhr and Ø. Grong. Acta Mater., 48 p.1605, 2000

(11). N. Saunders. J. Jpn Inst. Light Metals, 51(3) p.141, 2001

(12). O. R. Myhr and Ø. Grong. Acta Metall., 39 p.2693, 1991.

(13). M. J. Russell, H. R. Shercliff, and P. L. Threadgill, Aluminum Automotive and Joining Symposia; New Orleans, LA; USA; page 225. TMS, 2001.

(14). H. R. Shercliff, M. J. Russell, A. Taylor, and T. L. Dickerson. M´echanique and Industries, 6 p.25, 2005.

(15). T. Hyoe, P. A. Colegrove, and H. R. Shercliff. In Friction Stir Welding and Processing II as held at the 2003 TMS Annual Meeting; San Diego, CA; USA; 2-6 Mar., page 33. TMS, 2003.

(16). J. D. Robson, A. Sullivan, H. R. Shercliff, and G. McShane. TWI, UK. In Proc. 5th International Conference on Friction Stir Welding, 2004.

(17). D. Dumont, A. Deschamps, Y. Brechet, Acta Materialia, 52, p. 2529, 2004